Reports

Historical Nile Floods and Their Implications for Climatic Change

Abstract. *Analysis of Nile flood stages from A.D. 640 to 1921 reveals major episodes of low Nile discharge during the years 930 to 1070 and 1180 to 1350 and major episodes of high Nile floods during 1070 to 1180 and 1350 to 1470. Examination of Nile flood maxima and minima and comparison with water levels in Lake Chad reveal a correlation between high Nile discharge and greater rainfall in equatorial East Africa. There is also apparently a correlation between low Nile discharge and cold climate in Europe.*

Records of Nile flood stages dating back to the 7th century A.D. provide information that is useful for the study of recent climatic changes (*1–3*). So far, however, attempts to understand the implications of variations in Nile floods for climatic change have not been satisfactory (*4*). In the study reported here, Toussoun's (*5, 6*) compilation of Nile data was used, and the flood stages were corrected to their corresponding height above sea level by the Popper calibration method (*7*). Three different analytical techniques were used to detect episodic variations in flood stages. An attempt was made to determine the cause of the variations and to relate flood episodes to climate in Africa and Europe.

Temporal variations in Nile flood levels. The first method used to detect episodic variations in Nile floods is that of Kraus (*3, 8*). In this method deviations of flood heights (H) from a mean flood height ($\bar{H}$) are converted to deviations in flood discharge (V'). A normalized cumulative deviation (NCD) is obtained by dividing the sum of the deviations ($\Sigma V'$) by a mean flood discharge ($\bar{V}$)

$$\mathrm{NCD} = (\Sigma V')/\bar{V}$$

In the present analysis centennial averages of flood maxima were used to obtain the temporal trend of changes in flood maxima (*9*), and deviations of decadal averages of flood maxima from the trend values were determined. The deviations were accumulated and converted to cumulative discharge deviations by using the formula

$$V' = 57.49\ H'$$

where V' is the deviation in discharge in million cubic meters per day and H' is the deviation from the flood maximum. This formula is based on a regression equation obtained from the data on flood maxima (H) and discharge at Roda (V) by Willcocks (*9, 9a*):

$$V = 7.80.63 + 57.49\ H$$

The correlation coefficient for this relation is .93.

Instead of a constant mean discharge, the discharge obtained from the trend of centennial flood maxima was employed, obviating the need to assume a constant discharge through the centuries. The use of decadal averages of flood maxima also smooths the annual stochastic variations, and the calculation of deviations from the trend eliminates the problem of the rise of Nile bed as a result of siltation. The curve obtained by plotting the normalized cumulative deviations (Fig. 1A) indicates episodic fluctuations. A graph (Fig. 1B) based on a modified version of Alter's method for analyzing climatic data was also constructed (*10*). This is a plot of the mean difference (D) between observed decadal averages of the flood maxima, X_i and X_{i-L}, in a series, x_1, x_2, x_N, where L is the time interval between successive observation, or lag. The equation is

$$D = \frac{\sum^{N-1} (X_i - X_{i-1})}{N - L}$$

The value of D was multiplied by 100 to construct the Nile curve. The sign of D was not ignored to obtain a curve of cumulative deviations rather than a correlogram. The series of observations consist of the decadal changes of the flood maxima.

The third method used consists of determining the cumulative percentage differences (C) between successive observations, filtered by a weighted moving average (*11*). Decadal averages were converted to weighted moving five-point averages (*12*) to minimize irregular components. The smoothed series consisted of $B_1, B_2, \ldots, B_N$ values. The cumulative percentage difference was obtained from

$$C = \Sigma\left(\frac{B_i - B_{i-1}}{B_i}\right) \times 100$$

Table 1. Episodes of fluctuations in Nile flood levels.

This report		Bell (*13*)		Riehl and Meitín (*3*)	
Years A.D.	Nile floods	Years A.D.	Nile floods	Years A.D.	Nile floods
Before 650 to 1070	Generally low	760 to 1350	Generally low		
Before 650 to 700	Minor low	622 to 760	High	645 to 694	High
700 to 750	Minor high			714 to 803	High
750 to 790	Minor low				
790 to 830	Minor high			804 to 853	High
830 to 850	Minor low				
850 to 880	Minor high				
880 to 900	Minor low				
900 to 930	Minor high			897 to 956	High
930 to 1070	Major low	930 to 1080	Exceptionally low	957 to 1210	No fluctuations
1070 to 1180	Major high	1090 to 1190	High		
1180 to 1350	Major low	1200 to 1350	Exceptionally low	1210 to 1285	Low
1350 to 1470	Major high	1350 to 1470	Exceptionally high	1286 to 1467	Low
1470 to 1500	Minor low	1500 to 1522	High		
1500 to 1700	?	1522 to 1720	?		
1725 to 1800	Minor high	1738 to 1781	High	1725 to 1844	High
1800 to 1830	Minor low	1780 to 1839	Low		
1830 to 1870	Minor high	1840 to 1898	High	1844 to present	High

0036-8075/81/0605-1142$00.75/0

The curve in Fig. 1B and the cumulative percentage difference between moving averages (Fig. 1C) are closely matched. In addition, both are in general agreement with the $(\Sigma V')/\bar{V}$ curve.

The graphs show several Nile episodes. These are listed in Table 1 together with those previously inferred by Riehl and Meitín (3) and by Bell (13). Bell's results are in close agreement with mine.

Climatic interpretations. The Nile River receives its water from two major sources: the White Nile, which drains a large area of equatorial Africa, and the Ethiopian tributaries (14). The Ethiopian tributaries—the Atbara and the Blue Nile—are the major sources of Nile water. The Blue Nile delivers water at an annual average rate of 1620 m^3/sec, with as much as 5000 to 6000 m^3/sec during the flooding season. During that season, which begins in July and lasts until September, the contribution from the Ethiopian tributaries rises, reaching almost 100 percent by the end of August. The water level decreases after the flood and reaches a minimum in June, when the Nile is fed mostly by water from the White Nile and the contribution from the Ethiopian tributaries is as low as 25 percent (7, p. 248).

The seasonal distribution of rainfall in Ethiopia is commonly explained in terms of the position of the intertropical convergence zone (ITCZ), a low-pressure area of convergence between the tropical easterlies and the equatorial westerlies along which equatorial wave disturbance takes place. In broad terms, moist conditions prevail equatorward from the ITCZ and dry conditions occur poleward from it. In summer, the ITCZ is displaced southward in northeastern Ethiopia. In southeastern Ethiopia, air currents are in general southerly from the equatorial Indian Ocean. They are dry and subside after losing their moisture on the East African highlands. In the rest of Ethiopia, the influence of the Atlantic equatorial westerlies predominates. These air currents ascend over the Ethiopian highlands from the southwest and produce the main rainy monsoon season (15). In equatorial Africa between 5°N and 5°S the effect of the summer monsoons is weak and rainfall is bimodal in distribution (16).

Since the Nile flood maxima may thus be attributed to the monsoonal rains in Ethiopia and the flood minima mostly to rainfall in equatorial East Africa, analysis of the difference between the deviations from the decadal averages of the flood maxima and minima (17) may provide a clue to changes in wind circulation in the source area of the Nile. Accordingly, an index I_w was devised

$$I_w = \Sigma(dV_{\min,i} - dV_{\max,i})$$

Where $dV_{\min,i}$ and $dV_{\max,i}$ are the deviations from the average minimum and maximum discharges of the ith decade, respectively (17). This index measures the relative influence of the White Nile and hence the changes in precipitation in Ethiopia relative to equatorial East Africa, since 75 percent of the Nile water comes from the White Nile during the minima, compared with 100 percent from Ethiopia during the maxima. Incidentally, this measure is independent of siltation and can thus serve as an additional check on the validity of the climatic significance of the periods revealed by other methods.

The changes in I_w (Fig. 1E) match the variations exhibited in Fig. 1, A to C, before A.D. 1350; the periods of excess Nile flood discharge are correlated with positive values of I_w and vice versa, suggesting that short-term episodic vari-

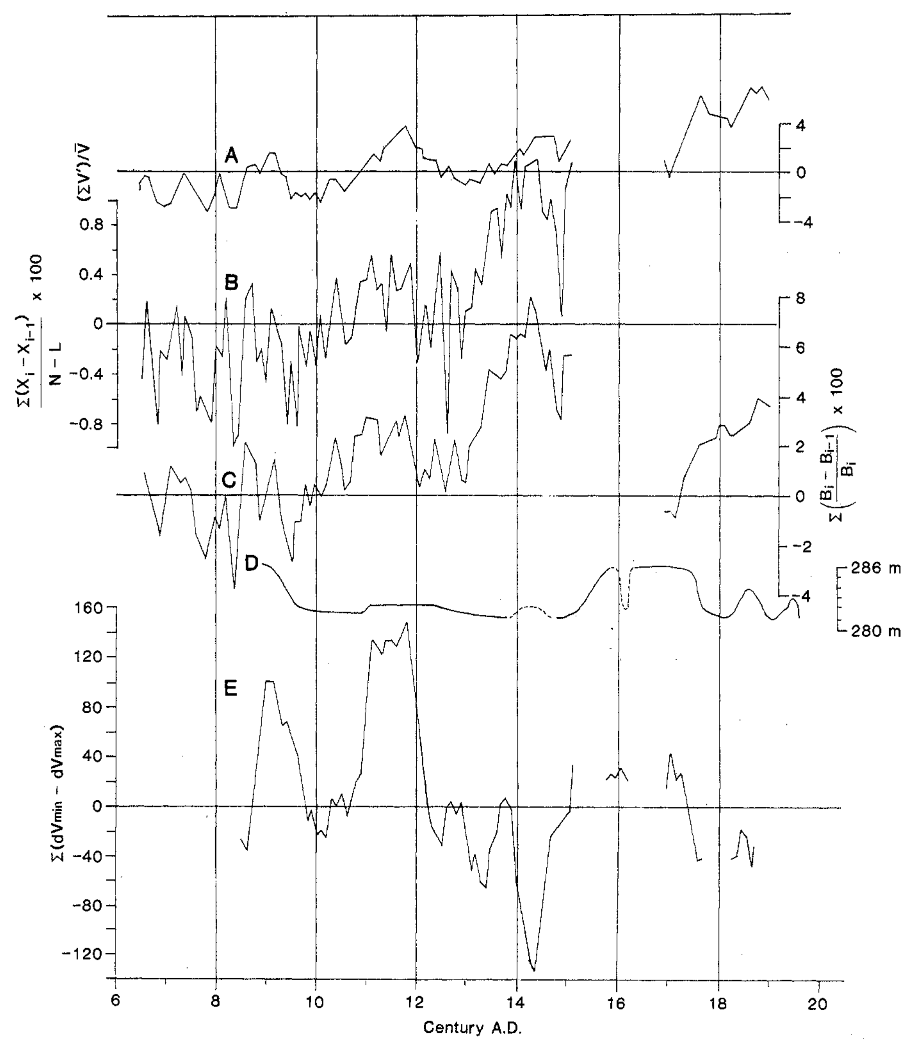

Fig. 1. (A) Cumulative normalized deviations $(\Sigma V')/\bar{V}$, where $\bar{V}$ is decadal discharge as determined from the trend of centennial averages of flood maxima, and V' is the deviation of decadal flood maximum from $\bar{V}$. The curve depicts episodic variations in flood discharge from A.D. 640 to 1921. Records from A.D. 1523 to 1700 are missing. (B) Episodic variation in Nile flood maxima as revealed by cumulative deviations of decadal averages (X_i) from those of the previous decade (X_{i-1}). The cumulative deviations are normalized by subdividing by the total number of decades (N) minus the time interval between successive observations (L). (C) Episodic variation in Nile flood maxima as revealed by cumulative deviations of flood maximum 10-year moving averages (five points, weighted) between successive decades $\Sigma(B_i - B_{i-1})$ subdivided by the 10-year moving average of the second decade in each pair (B_i). Note the similarity between episodic variations in (A), (B), and (C). (E) Cumulative difference between the deviations of flood maxima and flood minima, revealing the influence of water influx from equatorial tributaries (White Nile) relative to that from Ethiopian tributaries (Blue Nile and Atbara). The match with the other curves suggests that episodes of high Nile correspond in general to a relatively greater influence of equatorial sources. (D) Variations in water levels of Lake Chad (20). Note correspondence with (A) to (E). The match suggests that variations in Nile discharge are probably linked with climatic changes that influence rainfall in the basin of the White Nile and that of Lake Chad.

Fig. 2. Water level of Lake Chad (*20*) and decadal average of flood maxima from A.D. 1850 and 1920, showing remarkable similarity.

ations in Nile flood discharge are likely caused by relative increases in the contributions from the White Nile. The coincidence of low Nile levels in 1905 to 1915 (*5*, p. 404) with a low level of Lake Victoria (*18*) and the coincidence of relatively high levels of East African lakes during the second half of the 19th century (*18*) with a high discharge of the Nile at Aswan (*19*) supports this view. It is important to note here that there is a strong similarity between variations in Nile floods and variations in the water level of Lake Chad (Fig. 1D and Fig. 2) (*20*). It may thus be inferred that the episodic variations in Nile flood discharge are likely the result of climatic changes that influence precipitation in equatorial Africa.

The causes of climatic change in Africa are far from clear. Maley (*20*) attributes changes in the level of Lake Chad to shifts in the monsoons caused by the southern polar front from the Southern Hemisphere. Rognon and Williams (*21*) attribute climatic changes in North Africa to the effect of the jet stream of the westerlies, which influences the position of the subtropical anticyclone, which in turn affects the poleward movement of the ITCZ in summer.

Tanaka *et al.* (*22*) concluded that Sahelian rainfall patterns cannot be inferred from the position of the subtropical high over the Atlantic. They noted, however, a slight change in the morphology of the subtropical pressure belt and the trough of the mid-latitude westerlies. Drought coincides with increased solar heating at the surface due to decreased cloudiness and consequent changes in overall albedo. The rise in flow of the Ethiopian tributaries coincided with low radiation temperatures in 1974 (*23*).

The link between global climatic changes and Nile levels may also be considered in terms of the covariation of the Nile flood levels and paleoclimatic changes in Europe. The major climatic events during the time covered by the nilometer record in Europe are the "little or secondary climatic warm epoch" and the "Little Ice Age." The warm epoch is generally placed around A.D. 1150 to 1300 for most of Europe and the Little Ice Age around 1550 to 1700 (*2*, pp. 435 and 463). The Nile record for the period spanning the Little Ice Age is patchy, but evidence presented above and elsewhere (*24, 25*) indicates a low Nile from about 1470 to 1500 and 1640 to 1720. The record also indicates a number of low floods from 1674 to 1792, some of which left as much as two-thirds of Egypt unirrigated (*26*).

During the warm epoch, the Nile floods were characteristically high from 1070 to 1180 but low from 1180 to 1350. It is also interesting that the minor advance of glaciers from 1250 to 1300 (*2*, p. 463) is matched by a period of low Nile from 1180 to 1350, and that the most recent advance of glaciers in the Alps from 1800 to 1850 (*2*, p. 463) corresponds with a deficit in Nile discharge from 1780–1800 to 1830 [Fig. 1, A and C; see also figure 4 in (*21*)] and a drop in the level of Lake Chad (*20*, p. 196).

Examination of the Nile record before the 7th century A.D. is also instructive. Bell (*27*) noted that the level of the Nile fell from about 3050 to 2550 B.C. This coincided with a drop in lake levels in Ethiopia (*28*) and the end of a phase of expansion of the East African lakes by 3700 B.C. (*29*). There is circumstantial evidence (*30*) that the Nile floods were low during the First Intermediate Period, 2180 to 2130 B.C., and desiccation was noted at that time in the arid zone of North Africa (*21*, p. 318). This period of low Nile levels and climatic change in Africa corresponds to the early cooler phase of the Sub-Boreal period in Europe from 3300 to 2000 B.C. (*2*, p. 363). The correspondence between cold conditions in Europe and low Nile levels and vice versa may thus have been characteristic of the Holocene in general. Furthermore, the Atlantic period in Europe from about 6000 to 3000 B.C. (*2*, p. 372), which was one of the warmest postglacial periods, coincident with a moist phase in North Africa (*21*, p. 318) and high lake levels in East Africa. In Egypt, the levels of Birket Qarun Lake, which is fed by Nile floods, were high from 6000 to 5000 B.C. and had a minor rise again in 4200 B.C. (*31*).

Conclusions. Analysis of the record of Nile floods from A.D. 640 to the present reveals several short episodes of high and low floods. These short-term fluctuations in Nile flood maxima apparently reflect variations in the contributions from the White Nile and seem to match variations in water levels of Lake Chad connected with the poleward movement of the ITCZ. The episodes of low Nile discharge were probably synchronous with cold climate in Europe (*32*).

FEKRI A. HASSAN

Department of Anthropology,
Washington State University,
Pullman 99164

References and Notes

1. C. E. P. Brooks, *Climate Through the Ages* (Dover, New York, 1970), pp. 329–333.
2. H. H. Lamb, *Climate, Present, Past, and Future*, vol. 2, *Climate History and the Future* (Methuen, London, 1977), pp. 138–141 and 425–426.
3. H. Riehl and J. Meitín, *Science* **206**, 1178 (1979).
4. Data on annual Nile flood maxima and minima from A.D. 622 to 1921 were gleaned from original Arabic texts by Toussoun (*5*). The data were plotted by C. S. Jarvis [*Trans. Am. Soc. Civ. Eng.* **101**, 1012 (1936)], who also plotted 5-, 10-, and 100-year averages. Jarvis' plots were used by Riehl and Meitín (*3*) to detect episodic variation in Nile floods. However, the latter overlooked the original source of data and the critical examination of the Nile record by Popper (*1*), who showed that the flood stage data, as reported by Toussoun in meters above sea level, must be corrected since the units of measurements (cubit and fingers) were not constant through time.
5. O. Toussoun, "L'Histoire du Nil," *Mem. Inst. Egypte* 9 (1925), part 2.
6. O. Toussoun (*5*, part 2, pp. 366–404). The data consist of measurements of flood heights at the Roda nilometer, near Cairo. The nilometer was constructed in A.D. 715 (*6*, p. 16). Data going back to A.D. 622 were gathered from other nilometers in the neighborhood of Cairo by Arab scholars following the conquest of Egypt in A.D. 641 to 645 [S. I. Kashef, *Egypt at the Dawn of Islam* (Dar el-Nahda Al-'Arabia, Cairo, 1970), pp. 14–15 (in Arabic)]. However, the data from 622 to 640 are unreliable and are discounted in statistical treatments of the Nile record (*7*, pp. 165–190). The data used for the present analysis were obtained from the figures in cubits and fingers for the period A.D. 641 to 1921. Since these measurement units were not constant through time and the height of the nilometer above sea level was also variable, the primary data in cubits and fingers must be calibrated for these two sources of error. Popper's method (*7*, pp. 102–122) for calibrating the data to meters above sea level was used to obtain the figures for annual flood stages used here.

7. W. Popper, *The Cairo Nilometer* (Univ. of California Press, Berkeley, 1951).
8. E. B. Kraus, *Q. J. R. Meteorol. Soc.* **81**, 198 (1955).
9. The trend is primarily a result of the rise in channel bed as a result of siltation [J. Ball, *Contributions to the Geography of Egypt* (Government Press, Cairo, 1939), pp. 169–176]. The problem of Nile siltation was ignored in (*3*). W. Willcocks, *Egyptian Irrigation* (Spon, London, 1889), pp. 34–35.
10. E. T. Stringer, *Techniques of Climatology* (Freeman, San Francisco, 1971), pp. 92 and 434.
11. J. Shiskin, *Electronic Computers and Business Indicators* (National Bureau of Economic Research, New York, 1957).
12. A. B. Vistelius, *J. Geol.* **69**, 703 (1961).
13. B. Bell, in B. Bell and D. H. Menzel, *Toward the Observation and Interpretation of Solar Phenomena* (Air Force Cambridge Research Laboratories, Bedford, Mass., 1972). Bell took into account the conversions suggested by Popper and assumed a uniform rate of rise of the riverbed by 10 cm per century. She determined the deviations from the rising mean of flood levels and computed the cumulative deviations to infer the pattern of fluctuations in the volume of the Nile floods. The analysis by Riehl and Meitín (*3*) does not lead to detection of the major fluctuations from A.D. 930 to 1180–1190 shown by the analyses presented in this report and recognized by Bell. The major episodes of low Nile floods in A.D. 1180–1200 to 1350 inferred in this report and by Bell are recognized by Riehl and Meitín, although they place the termination of that episode 65 years earlier. The low which they find between 1286 and 1467 is detected as a period of exceptionally high floods here and by Bell. K. W. Butzer brought Bell's analysis to my attention.
14. H. E. Hurst, *The Nile* (Constable, London, 1957); M. Awad Mohamed, *The River Nile* (Lagnat al-Talif wa-Targama wa-Nashr, Cairo, 1952) (in Arabic).
15. D. Gamachu, *Aspects of Climate and Water Budget in Ethiopia* (Addis Ababa Univ. Press, Addis Ababa, 1977), pp. 4–5.
16. C. S. Ramage, *Monsoon Meteorology* (Academic Press, New York, 1971), pp. 16 and 128; M. Awad Mohamed, in *ibid.*, pp. 212–214.
17. Original data from (*7*), p. 180.
18. T. W. Butzer, *Recent History of an Ethiopian Delta* (Univ. of Chicago Press, Chicago, 1971).
19. E. B. Kraus, *Q. J. R. Meteorol. Soc.* **82**, 96 (1956).
20. J. Maley, *Paleogeogr. Paleoclimatol. Paleoecol.* **14**, 193 (1973).
21. P. Rognon and M. A. J. Williams, *ibid.* **21**, 285 (1977).
22. M. Tanaka, B. C. Weare, A. R. Navato, R. E. Newell, *Nature (London)* **255**, 201 (1975).
23. H. Riehl, M. El-Bakry, J. Meitín, *Mon. Weather Rev.* **107**, 1546 (1979).
24. A. Zakry, *The Nile in the Pharaonic and Islamic Period* (Matb'et Al Ma'arif, Cairo, 1926), pp. 52–53 (in Arabic).
25. P. J. Mehringer, Jr., K. L. Petersen, F. A. Hassan, *Quat. Res. (N.Y.)* **11**, 238 (1979).
26. A. Zakry (*24*, p. 59); O. Toussoun (*5*, pp. 501–503). A period of low Nile discharge from 1700 to 1740 is also shown by the analysis in (*23*).
27. B. Bell, *Geogr. J.* **136** (part 4), 569 (1970).
28. M. A. J. Williams, P. M. Bishop, F. M. Dakin, R. Gillespie, *Nature (London)* **267**, 690 (1977); F. Gasse and P. Rognon, *Rev. Geogr. Phys. Geol. Dyn.* **2**, 405 (1973); F. Gasse, *Nature (London)* **265**, 42 (1977); F. A. Street and A. T. Grove, *ibid.* **261**, 387 (1976).
29. K. W. Butzer, G. L. Isaac, J. L. Richardson, C. Washbourn-Kamau, *Science* **175**, 1069 (1972). K. W. Butzer (*Phys. Geogr.* **1**, in press) notes a high stand of Lake Rudolf at 4500 to 2000 B.C.
30. B. Bell, *Am. J. Archaeol.* **75**, 1 (1971); K. W. Butzer, in *The Causes and Consequences of Food Production in Africa*, J. D. Clark and S. A. Brandt, Eds. (Univ. of California Press, Berkeley, 1980).
31. F. Wendorf and R. Schild, *Prehistory of the Nile Valley* (Academic Press, New York, 1976), pp. 222–226.
32. A similar conclusion was reached by D. A. Adamson, F. Gasse, F. A. Street, and M. A. J. Williams [*Nature (London)* **288**, 50 (1980)]. They inferred minimum water yield during the very cold late Pleistocene interval.
33. Supported by grants from the National Science Foundation (BNS 78-08177) and the Foreign Currency Program, Smithsonian Institution (FC 80-662700). I thank K. W. Butzer, B. Bell, P. J. Mehringer, Jr., and K. Petersen, who read the manuscript and made useful suggestions.

24 June 1980; revised 19 December 1980

Origins of Chirality in Nature: A Reassessment of the Postulated Role of Bentonite

Abstract. *Bondy and Harrington have proposed that selective binding of* L *isomers of amino acids and* D *isomers of sugars to bentonite is the mechanism by which the chirality of molecules in living cells was originally established. Further experiments indicate that the observations of Bondy and Harrington are better explained in terms of the effects of the binding to bentonite of the products of radiochemical decomposition.*

Recently (*1*) Bondy and Harrington described experiments that they interpreted as showing preferential binding to bentonite of the L isomers of amino acids (thus suggesting a possible origin of chiral molecules in nature). We have not been able to confirm a preferential binding of the L isomers of amino acids, and experiments described here suggest that the radioactivity bound to bentonite is largely due to the binding of radiochemical decomposition products.

Tritiated compounds are usually supplied at 98 to 99 percent purity, but they may have rates of decomposition as high as 1 percent per month. The products of decomposition "stick" to any insoluble macromolecules. It has been suggested that measurements of bound radioactivity should be expressed as a percentage of the total counts available to make it clear when the observed binding is within the range of the concentration of impurities (*2*). Results are quoted here in this form as well as in the form of picomoles per 10 mg of bentonite for comparison with the data of Bondy and Harrington. From their data the percentage of available counts bound was calculated. In most instances, these values were 4 percent or less. The exception was the binding of L-[^{3}H]leucine, for which the percentage bound was 45 percent at a concentration of $10^{-8}M$. This was not in agreement with the published dissociation constant of $4.6 \times 10^{-6}M$, which implies that 50 percent binding was reached only at a concentration 460 times higher. Bondy (*3*) has said that 45 percent binding was not observed at $10^{-8}M$, and he thought the figure should have been one-tenth of this amount. It is probably worth noting that Bondy and Harrington used L-leucine at a specific activity of 58 Ci/mmole and D-leucine at 1 Ci/mmole because at higher specific activity tritiated compounds are less stable (*2*).

The ^{3}H-labeled amino acids that we used were obtained from the Radiochemical Centre, Amersham. These were L-aspartic acid (15 Ci/mmole), D-aspartic acid (18 Ci/mmole), L-leucine (55 Ci/mmole), and DL-leucine (42 Ci/mole). Unfortunately, D-[^{3}H]leucine was no longer available. The use of DL-leucine meant that, if D-leucine were not bound at all, the counts bound with DL-leucine would be 50 percent of those bound with L-leucine of the same concentration. In Bondy and Harrington's data, D-leucine was bound to 15.3 percent the extent of L-leucine. With DL-leucine, an equivalent result would require the binding to be 57.7 percent of that of L-leucine. Unlabeled amino acids were obtained from Sigma Chemical Company.

Three samples of bentonite were obtained by courtesy of Volclay from their sites at Lovell, Upton, and Belle Fourch. One sample of Queensland bentonite was supplied by Minerals Ltd. (Australia). These samples were washed with hot alkali as described by Bondy and Harrington (*1*). In the washing process gritty contaminants were removed, and by centrifugation coarser and finer particles of bentonite were separated. The finer particles had a swollen diameter of 1 to 1.5 μm. The binding of counts by fine and coarse particles of bentonite was similar, an indication that the phenomenon is related to the mass or volume of the swollen particles rather than to the surface area.

Bentonite suspensions were dispersed by volume with a reproducibility of 3 percent in the counts bound to 10 mg of bentonite. Despite the alkaline wash, we found it necessary to sterilize the bentonite and dispense it aseptically. Otherwise, microbial growth on bentonite resulted in preferential binding of the L-aspartic acid as compared with D-aspartic acid. Similarly, the dilute solutions of ^{3}H-labeled amino acids were freshly prepared with aseptic precautions because, when a diluted solution was stored at 2°C for a week, an increase in binding of L-aspartic acid (from 0.2 to 0.6 percent) was observed. To minimize the differences between our procedures and those of Bondy and Harrington, we used 50 m*M* tris-HCl buffer (*p*H 7) after we found that binding was similar in other salt solutions and only somewhat reduced in water.

Counting of the supernatants of the bentonite suspensions established that the percentage of counts bound was too